

# Zircon U-Pb chronology and geochemistry of porphyritic granites: A case study of the Dalancun granites in Zhaoyuan, Shandong Province

Renshun Jiang

Shandong University of Science and Technology

Jiang95082895@163.com

**Abstract.** The granite in Dalancun, Zhaoyuan, Shandong Province is mainly porphyry granite. In this paper, detailed field geology, petrology, isotopic chronology and whole-rock principal and microgeochemistry have been studied. LA-ICP-MS zircon U-Pb chronology shows that it was formed in the Early Cretaceous ( $129.7 \pm 0.8$  Ma), later than Linglong granite (160-150 Ma) and earlier than Laoshan granite (120-114 Ma). It is consistent with the main ore-forming age of Jiaodong large gold deposit and the diagenetic age of Guojialing granite (130-126 Ma).  $K_2O+Na_2O=7.41\% \sim 9.37\%$ ,  $K_2O/Na_2O=0.78 \sim 1.24$ ;  $A/CNK=0.89 \sim 1.06$ ,  $MgO=0.63\% \sim 1.01\%$ , with high K, Al characteristics, belongs to the quasi-aluminum-peralumin high potassium calc-alkaline series. The strong differentiation of rare earth elements (La/Yb)  $N=68.24 \sim 93.96$ , weak positive Eu anomaly ( $\delta Eu=1.26 \sim 1.769$ ), enrichment of large ion lithophile elements Ba, Sr, high field strength elements Nb, Ta, Ti deficit, indicating the geochemical characteristics of continental lithosphere. In addition, high Sr ( $1817 \times 10^{-6} \sim 2017 \times 10^{-6}$ ), low Y ( $7.55 \times 10^{-6} \sim 9.36 \times 10^{-6}$ ), Sr/Y ratio between 199.89~262.29, Nb/Ta ratio between 14.67~16.73, consistent with continental crust ratio, It shows the characteristics of type I granite and Adakite. Combined with other geochemical indexes and regional geological studies, this paper suggests that the Dellancun porphyritic granite belongs to crust-mantle granite, which may have been formed in the arc environment of continental margin during the transition from compressive to extensional tectonic system in Jiaodong area, and is closely related to the subduction of the paleo-Pacific plate. This study not only helps to understand the Mesozoic tectonic evolution in eastern China, but also provides a basis for revealing the formation mechanism of Jiaodong gold deposit.

**Keywords:** Zircon U-Pb chronology; Geochemistry; Adakite; Tectonic environment, Jiaodong Peninsula.

## 1. Introduction

Jiaodong Peninsula is located in the eastern margin of North China Craton and is mainly composed of Jiaobei Terrane and Sulu Terrane. Jiabei terrane includes Jiabei uplift in the north and Jiaolai Basin in the south [1-3]. During the destruction of the North China Craton, Mesozoic magmatic activity was strong in eastern China and a large amount of granite was developed. There are many types of granite, mainly porphyritic - porphyritic, ovoid - spherical, etc. [4-7]. At the same time, the development of granite is accompanied by the enrichment and mineralization of large vein type and hydrothermal type gold and other precious metal elements, forming the largest gold deposit in Jiaodong area of China - Zhaoyuan gold deposit, and the gold deposit is mainly developed in the late Jurassic-Early Cretaceous granite. There are two views on the genesis of the early Cretaceous granite in North China: (1) the mixing of crust and mantle under the Paleo-Pacific plate subduction background and the subsequent delamination [8]; (2) Partial melting of thickened continental crust [9]. Among them, porphyritic - porphyritic granite has attracted much attention due to its characteristic structure and specific tectonic environment [10]. Based on the above, this paper takes the porphyritic granite in Zhaoyuan area of Shandong province as the research object, and carries out detailed field geology, petrology, isotope chronology and whole-rock principal and micro geochemistry studies, and defines the crystallization age, rock genesis and tectonic environment of the granite.

## 2. Regional geological overview and petrographic characteristics

The research area is located in Dalan Village, Zhaoyuan City, Yantai City, north Jiaodong Peninsula. The Mesozoic granites in Jiabei area are mainly distributed to the east of Tanlu fault and were formed in the Late Triassic, Late Jurassic and Early Cretaceous respectively (FIG. 1). The Late Triassic granite only appears in the Jiazishan - Cha Shan area. Late Jurassic granite distributed in Jiabei uplift in the form of rock base. Early Cretaceous granite is widely distributed in the eastern Tanlu fault. Among them, the early Cretaceous granites in Jiabei uplift interspersed between or along the margin of Late Jurassic granites with beads and dikes, and showed basal outcrops in Jiaonan area. According to the formation age of early Cretaceous granite, it can be further divided into three types: Early Cretaceous Linglong type, middle Early Cretaceous Guojialing type and late Early Cretaceous Laoshan type. Among them, Linglong type and Guojialing type granites are believed to be closely related to the genesis of Jiaodong large gold deposit<sup>[11-18]</sup>.

Surrounded by Linglong type granite (160-150 Ma), Dellancun porphyritic granite is produced in the form of rock strains, with an outcrop of about 50km<sup>2</sup>. It is nearly circular in plane. The contact boundary is controlled by two groups of NE-NW faults, the inner contact zone is developed by ductile shear, and Linglong granite fragments are wrapped in the middle. The porphyritic granite in Dalanvillage is mainly composed of amphibolite monzogranite, and the dark xenoliths can be seen sporadically in the rock mass. The contact line between the porphyritic granite and the rock mass is clear with a condensed edge. In this study, the analysis and test samples were collected from the southern part of the rock mass (N37°30 '52 " , E120°22' 14 " ). The samples were fresh and did not suffer from strong weathering and late hydrothermal alteration (Figure 2).

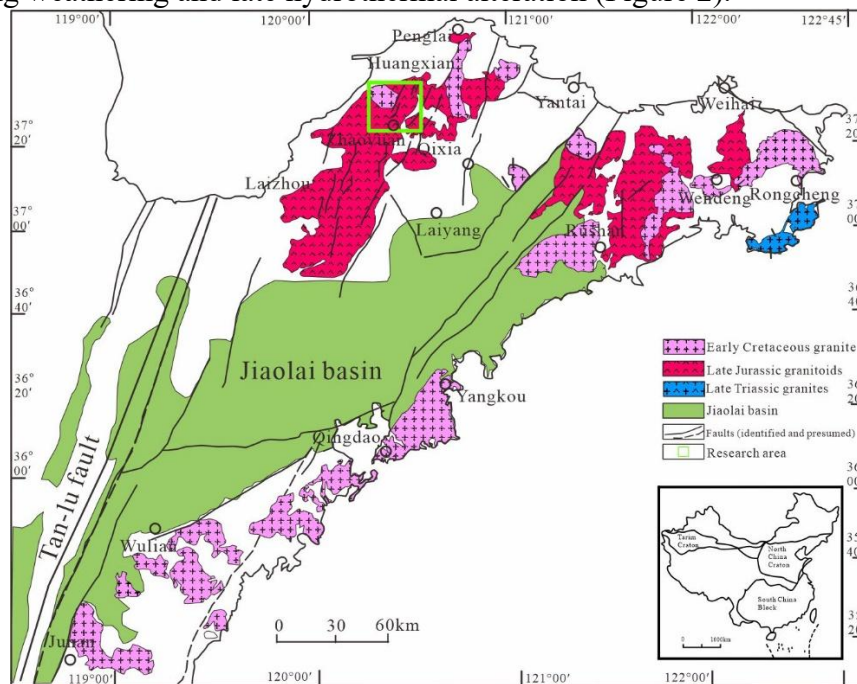


Fig. 1 Regional geological map of Jiaodong area<sup>[19]</sup>

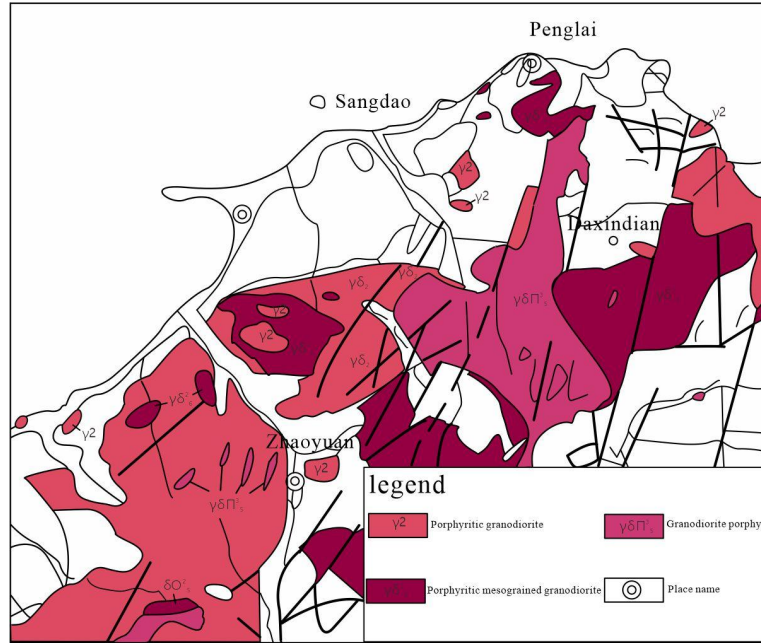


Fig. 2 Geological map and sampling location map of granite in Dalan Village

Amphibolite monzogranite is gray - white, medium - coarse-grained porphyritic structure, massive structure. The plagioclase (40%) is heteromorphic to hemiautidiomorphic plate,  $\phi=0.15\times0.2\sim1.6\times3.5\text{mm}$ ; Potassium feldspar (35%) is heteromorphic,  $\phi=0.6\times0.8\sim4.0\times7.5\text{mm}$ ; Quartz (23%) is heteromorphic granular,  $\phi=0.1\times0.2\sim1.0\times3.0\text{mm}$ ; The common amphibole (30%) is semi-autogenous granular columnar, incomplete columnar,  $\phi=0.15\times0.2\sim0.6\times1.5\text{mm}$ ; The secondary minerals are flake granular biotite (3%),  $\phi=0.1\times0.15\sim0.8\times1.5\text{mm}$ ; The sub-minerals are zircon, apatite, sphene, and so on (Figure 3).

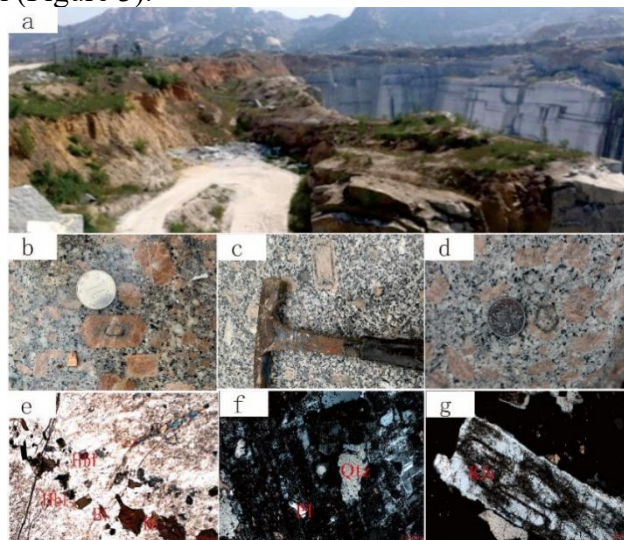


Fig. 3 Outcrop and micrograph of granite in Dalan Village

### 3. Sample profile and test method

A total of 10 granite samples were collected in this paper, and one granite sample (DDR10) was dated by LA-ICP-MS U-Pb. The remaining 9 samples (DLC-01 -- DLC-09) were analyzed by X-ray fluorescence spectrometer and plasma mass spectrometer, respectively. The above experiments were done in the State Key Laboratory of Continental Dynamics, Northwest University. The laser denudation system is a GeoLas200M laser (Ar F-excimer with a wavelength of 193nm) produced by Lambda physik, Germany. Helium is used as carrier gas, the beam aperture is 20 $\mu\text{m}$ ,

the denudation depth is 20~40 $\mu\text{m}$ , the laser frequency is 10Hz, and the energy is 0.032~0.036J. During the test, nitrogen was added into the plasma central flow to improve the instrument sensitivity, reduce the detection limit and improve the analytical precision<sup>[20]</sup>. Standard zircons GJ1 (600 Ma) and 91500 (1064Ma) were used as external reference materials for zircon ages, NIST SRNI610 was used as external standard for element content, and <sup>29</sup>Si was used as internal standard element for calibration. The off-line processing of analytical Data (including selection of samples and blank signals, calibration of instrument sensitivity drift, element content, U-Th-Pb isotope ratio and age calculation) was completed by ICPMS Data Cal<sup>[21]</sup>. Detailed instrument operating conditions are the same as Liu et al.<sup>[22-23]</sup>, and GLITTER4.4 is adopted as the data processing software. Zircon U-Pb harmonic maps and calculated weighted flat maps were plotted using ISOPLOT program (Ver3.23)<sup>[24]</sup>. Standard sample 91500 was used for external calibration of isotope composition, and the detailed analysis method of LA-ICP-MS was described in literature<sup>[25-26]</sup>.

## 4. Analyze the results

### 4.1 Zircon U-Pb Chronology Analysis

The zircons in the samples are mostly euhedral to hemihedral, with clear magmatic growth zones (FIG. 4), and Th/U ratios of the zircons are all between 0.44 and 1.05 (Table 1), suggesting that these zircons are all magmatic zircons. 40 zircons from LCC-10 were analyzed, and 32 sets of effective zircon ages were obtained. The <sup>6</sup>Pb/<sup>238</sup>U congruent ages ranged from 133.9 to 126.2Ma, with a weighted mean age of  $129.7 \pm 0.8$  Ma (MSWD=1.2, n=32) (FIG. 5). It represents the emplacement crystallization age of Dellancun porphyritic granite, which is early Cretaceous.

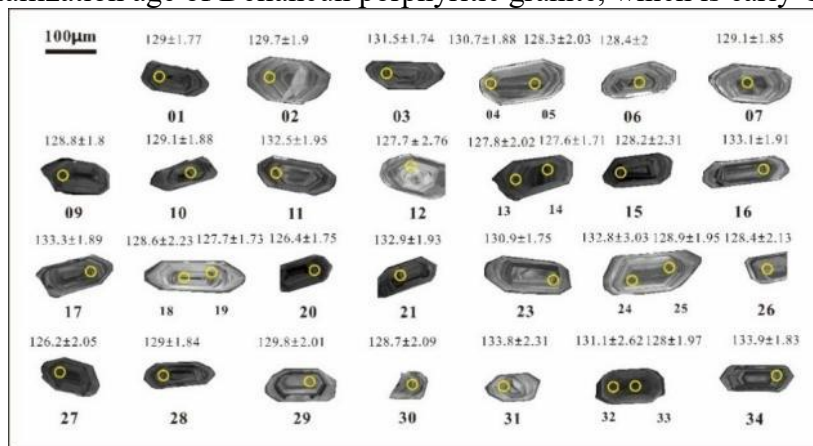


Fig. 4 Representative zircon CL cathode luminescence diagram of Dellancun granite

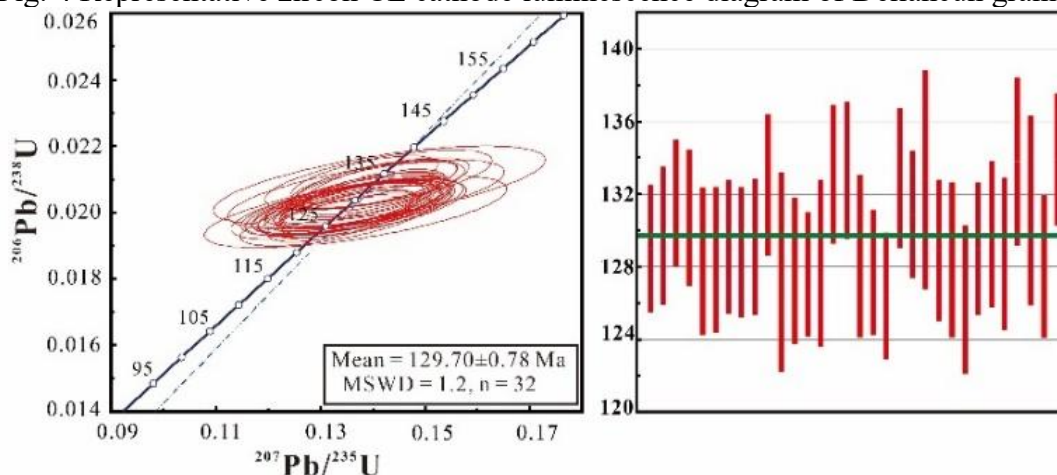


Fig. 5 Zircon U-Pb age map of the granite in Dalancu

Table 1 Statistical table of LA-ICP-MS U-Pb age data of zircon from Dalancun granite

serial number	content (10 <sup>-6</sup> )			Isotope ratio						Age /Ma					
	Th	U	Th/U	207Pb/206Pb	1 σ	207Pb/235U	1 σ	206Pb/238U	1 σ	207Pb/206Pb	1 σ	207Pb/235U	1 σ	206Pb/238U	1 σ
01	456	625	0.73	0.0489	0.002	0.1363	0.006	0.0202	0.0003	142.5	101.5	129.7	4.9	129.0	1.8
02	243	552	0.44	0.0496	0.003	0.139	0.007	0.0203	0.0003	176.4	116.9	132.1	6.0	129.7	1.9
03	363	615	0.59	0.0493	0.002	0.1403	0.005	0.0206	0.0003	163.7	97.9	133.3	4.9	131.5	1.7
04	309	594	0.52	0.0491	0.002	0.1387	0.006	0.0205	0.0003	152.1	113.3	131.9	5.7	130.7	1.9
05	366	458	0.8	0.0487	0.003	0.1351	0.007	0.0201	0.0003	133.7	131.3	128.6	6.6	128.3	2.0
06	473	717	0.66	0.0488	0.003	0.1354	0.007	0.0201	0.0003	138.3	126.8	129.0	6.4	128.4	2.0
07	265	308	0.86	0.0496	0.003	0.1384	0.007	0.0202	0.0003	176.4	116.0	131.6	5.9	129.1	1.9
09	514	745	0.69	0.049	0.002	0.1364	0.006	0.0202	0.0003	147.2	106.2	129.8	5.2	128.8	1.8
10	519	494	1.05	0.049	0.002	0.1366	0.006	0.0202	0.0003	147.3	114.4	130.0	5.7	129.1	1.9
11	292	400	0.73	0.0492	0.003	0.141	0.007	0.0208	0.0003	158.0	117.3	133.9	6.1	132.5	2.0
12	248	243	1.02	0.0496	0.004	0.1367	0.012	0.0200	0.0004	173.8	196.7	130.1	10.5	127.7	2.8
13	373	678	0.55	0.0496	0.003	0.137	0.007	0.0200	0.0003	176.3	128.7	130.3	6.6	127.8	2.0
14	368	504	0.73	0.0489	0.002	0.1347	0.005	0.0200	0.0003	141.1	99.8	128.3	4.8	127.6	1.7
15	444	705	0.63	0.0489	0.003	0.1354	0.009	0.0201	0.0004	141.8	159.1	129.0	8.2	128.2	2.3
16	587	903	0.65	0.0489	0.002	0.1407	0.006	0.0209	0.0003	143.6	110.9	133.7	5.6	133.1	1.9
17	453	708	0.64	0.0496	0.002	0.143	0.006	0.0209	0.0003	176.6	108.6	135.7	5.6	133.3	1.9
18	590	766	0.77	0.049	0.003	0.136	0.009	0.0202	0.0004	146.0	150.3	129.5	7.7	128.6	2.2
19	513	802	0.64	0.0491	0.002	0.1355	0.005	0.0200	0.0003	152.9	99.8	129.0	4.8	127.7	1.7
20	587	815	0.72	0.0489	0.002	0.1335	0.006	0.0198	0.0003	141.3	104.2	127.2	5.0	126.4	1.8
21	564	773	0.73	0.0488	0.002	0.1402	0.006	0.0208	0.0003	137.7	113.9	133.2	5.8	132.9	1.9
23	406	712	0.57	0.0493	0.002	0.1396	0.005	0.0205	0.0003	164.2	98.0	132.7	4.9	130.9	1.8
24	433	656	0.66	0.0492	0.005	0.1413	0.013	0.0208	0.0005	157.9	208.6	134.2	11.5	132.8	3.0
25	402	670	0.6	0.049	0.003	0.1363	0.007	0.0202	0.0003	145.9	124.0	129.8	6.2	128.9	2.0
26	360	571	0.63	0.0489	0.003	0.1356	0.008	0.0201	0.000	141.8	143.6	129.1	7.3	128.4	2.1

									3						
27	362	658	0.55	0.0488	0.003	0.133	0.007	0.0198	0.000 3	138.4	135.0	126.8	6.7	126.2	2.1
28	501	677	0.74	0.0489	0.002	0.1364	0.006	0.0202	0.000 3	143.6	110.6	129.8	5.5	129.0	1.8
29	457	714	0.64	0.0489	0.003	0.1372	0.007	0.0203	0.000 3	144.8	127.9	130.6	6.5	129.8	2.0
30	464	748	0.62	0.0489	0.003	0.136	0.008	0.0202	0.000 3	143.1	136.5	129.4	6.9	128.7	2.1
31	404	709	0.57	0.0488	0.003	0.1411	0.009	0.0210	0.000 4	138.3	148.9	134.0	7.9	133.8	2.3
32	411	709	0.58	0.049	0.004	0.1387	0.011	0.0206	0.000 4	146.2	180.0	131.9	9.6	131.1	2.6
33	302	305	0.99	0.0491	0.003	0.1357	0.007	0.0201	0.000 3	151.3	128.4	129.2	6.5	128.0	2.0
34	501	808	0.62	0.0478	0.002	0.1384	0.006	0.0210	0.000 3	89.1	105.5	131.6	5.1	133.9	1.8

## 4.2 Characteristics of major elements

Dalancun porphyritic granite  $\text{SiO}_2=68.98\% \sim 72.01\%$  (mean 69.88%),  $\text{Na}_2\text{O}=3.73\% \sim 4.84\%$  (mean 4.38%),  $\text{K}_2\text{O}=3.56\% \sim 4.77\%$  (mean 4.15%);  $\text{K}_2\text{O}+\text{Na}_2\text{O}=7.41\% \sim 9.37\%$  (mean 8.53%);  $\text{K}_2\text{O}/\text{Na}_2\text{O}=0.78 \sim 1.24$  (mean 0.96);  $\text{Al}_2\text{O}_3=14.64\% \sim 15.37\%$  (mean 15.16%);  $\text{A}/\text{CNK}=0.89 \sim 1.06$ , which is between quasi-aluminum and peraluminum.  $\text{MgO}=0.63\% \sim 1.01\%$  (mean 0.81%);  $\text{CaO}=1.76\% \sim 2.65\%$  (mean 2.25%);  $\text{TiO}_2=0.21 \sim 0.29\%$  (mean 0.25%) (Table 2). In the TAS classification map, the samples fall in the granite and quartzite syenite regions (FIG. 6). In the diagram of  $\text{SiO}_2\text{-K}_2\text{O}$ , the sample falls in the high potassium calc-alkaline region (FIG. 6a). In the  $\text{SiO}_2\text{-}(\text{K}_2\text{O}+\text{Na}_2\text{O})$  diagram, the sample falls in the transition zone between granite and quartz monzonite (FIG. 6b). In the  $\text{A}/\text{CNK}\text{-A}/\text{NK}$  diagram, most of the samples were located in the quasi-aluminous region, and a few were located in the peraluminous region (FIG. 6c). In the  $\text{A.R.}\text{-SiO}_2$  diagram, most samples are located in the alkaline region, and a small amount are located in the calc-alkaline region (FIG. 6d). To sum up, the porphyry amphibolite monzogranite in Dalancun belongs to the quasi-aluminous - peraluminous high potassium calc-alkaline series.

Table 2 Data Table of major elements of porphyritic granite in Dellancun (wt%)

	DLC-1	DLC-2	DLC-3	DLC-4	DLC-5	DLC-6	DLC-7	DLC-8	DLC-9
$\text{SiO}_2$	68.98	69.00	71.19	69.42	69.66	72.01	69.19	69.43	70.01
$\text{Al}_2\text{O}_3$	15.37	15.08	15.14	15.24	15.49	14.64	15.04	15.18	15.25
$\text{TFe}_2\text{O}_3$	1.67	2.12	1.48	1.71	1.76	1.73	1.90	1.78	1.94
$\text{MgO}$	0.75	1.01	0.63	0.78	0.81	0.85	0.87	0.82	0.77
$\text{CaO}$	2.30	2.65	1.76	2.01	2.15	2.02	2.55	2.50	2.34
$\text{Na}_2\text{O}$	4.60	4.65	3.73	4.24	4.07	3.85	4.82	4.84	4.62
$\text{K}_2\text{O}$	4.77	3.97	4.63	4.50	4.57	3.56	3.93	3.86	3.59
$\text{MnO}$	0.02	0.03	0.02	0.02	0.02	0.02	0.03	0.03	0.02
$\text{TiO}_2$	0.25	0.27	0.21	0.22	0.22	0.25	0.29	0.28	0.28
$\text{P}_2\text{O}_5$	0.10	0.13	0.10	0.12	0.11	0.10	0.13	0.12	0.12
LOI	0.54	0.51	0.50	1.12	0.53	0.45	0.67	0.61	0.53
$\text{FeO}$	1.03	1.19	0.94	1.00	1.03	1.21	1.13	1.02	1.17
Total	99.34	99.43	99.39	99.41	99.39	99.49	99.42	99.44	99.47

A/CN K	0.91	0.90	1.05	0.98	1.00	1.06	0.89	0.91	0.97
A/NK	1.21	1.26	1.36	1.28	1.33	1.44	1.23	1.25	1.33
A.R.	3.25	2.89	2.95	3.05	2.92	2.60	2.98	2.94	2.75

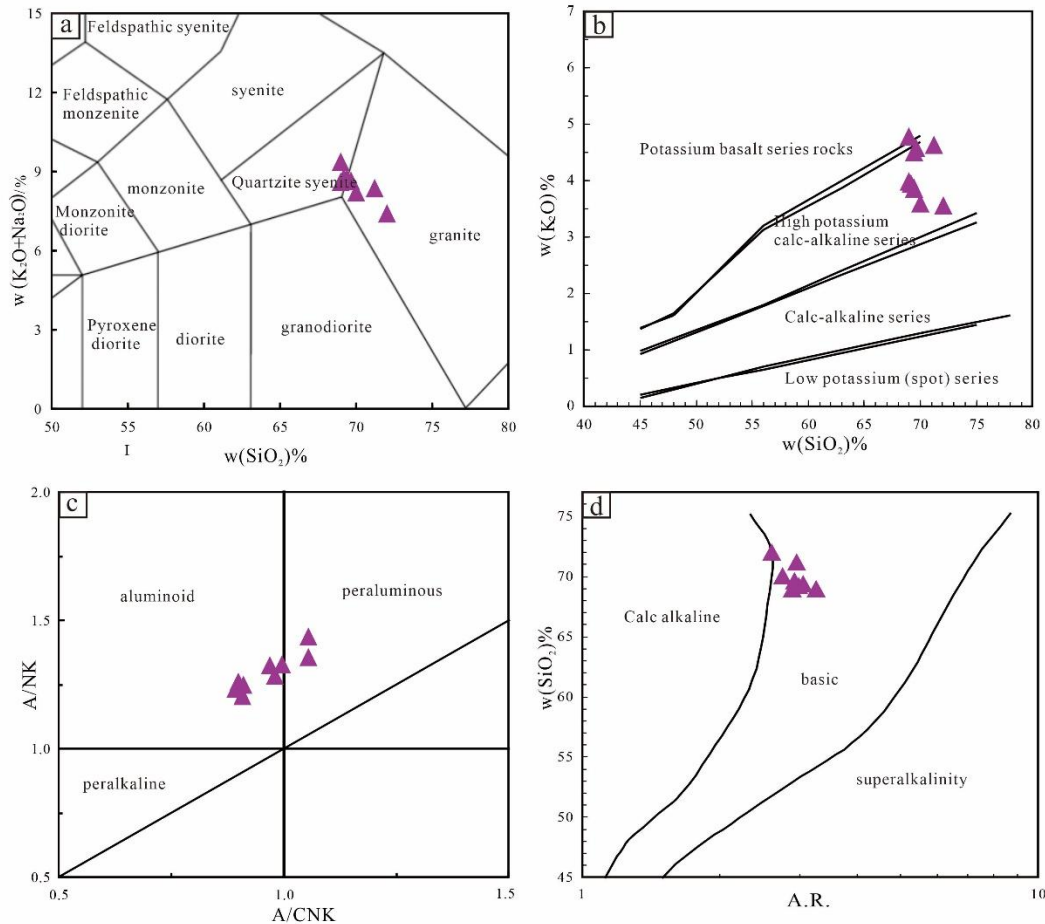


Fig. 6. Classification of porphyritic granite rocks and discrimination diagram of rock series in Dellan Village<sup>[27-30]</sup>

**4.3 Characteristics of trace elements**

$\Sigma REE=251.84 \times 10^{-6} \sim 326.40 \times 10^{-6}$  (average  $286.67 \times 10^{-6}$ ), (La/Sm)  $N=6.20 \sim 8.08$ , indicating extreme enrichment of LREE (Table 3). Samples  $Yb=0.60 \times 10^{-6} \sim 0.74 \times 10^{-6}$  (mean  $0.68 \times 10^{-6}$ ), (La/Yb)  $N=68.24 \sim 93.96$ , REE chondrite partition pattern of right-leaning, light REE enrichment, light and heavy REE strong differentiation.  $\delta Eu=1.26 \sim 1.769$  (mean 1.45), Eu showed a weak positive anomaly. The enrichment of large ion lithophile elements (LILE) Ba and Sr, and the depletion of high field strength elements (HFSE) Nb, Ta, Ti, indicate that it has the geochemical characteristics of continental lithosphere.

Table 3 Data table of trace elements of porphyry granite in Dellancun ( $10^{-6}$ )

	DLC-1	DLC-2	DLC-3	DLC-4	DLC-5	DLC-6	DLC-7	DLC-8	DLC-9
Sc	7.74	8.52	6.87	7.24	7.36	7.22	8.09	6.07	6.50
Cr	16.3	23.2	17.2	20.1	20.5	20.8	18.1	17.4	18.8
Co	2.98	3.89	3.09	3.20	3.47	3.89	3.45	3.27	3.51
Ga	21.5	22.2	21.9	21.2	21.8	22.6	22.7	22.3	22.8

Rb	81.7	74.8	94.3	90.3	88.3	79.6	75.6	76.5	75.9
Sr	1953	1870	2017	1817	1998	1938	1871	1899	1869
Zr	119	94.4	89.5	102	92.9	102	130	133	110
Nb	5.72	6.12	5.72	5.58	5.71	6.78	7.13	6.67	6.73
Cs	1.23	1.35	1.15	1.19	1.40	1.11	1.81	1.35	1.13
Ba	4090	3309	4804	4010	4433	3808	3272	3067	3167
Hf	3.23	2.68	2.52	2.82	2.59	2.90	3.56	3.66	3.05
Ta	0.39	0.40	0.38	0.35	0.38	0.43	0.46	0.43	0.40
Pb	33.1	31.7	37.4	33.2	35.6	33.2	31.7	32.6	33.1
Th	13.1	12.8	12.2	13.8	11.5	13.5	13.4	15.2	15.8
U	1.96	1.30	1.43	2.79	1.31	1.46	3.85	2.14	1.55
Y	7.55	8.78	7.69	7.91	7.93	8.89	9.36	8.46	8.29
La	72.1	74.8	69.5	82.1	66.2	80.4	73.9	79.6	91.2
Ce	120	126	117	135	112	133	127	133	146
Pr	13.3	13.9	13.0	14.5	12.5	14.6	14.4	14.7	15.8
Nd	44.8	47.5	44.2	47.9	42.4	49.0	49.9	49.6	51.8
Sm	6.34	6.99	6.42	6.62	6.26	7.06	7.44	7.11	7.05
Eu	3.07	2.92	3.56	3.16	3.16	3.17	2.93	2.78	2.88
Gd	5.87	6.42	5.90	6.37	5.51	6.43	6.45	6.39	6.67
Tb	0.56	0.62	0.57	0.58	0.55	0.63	0.65	0.61	0.62
Dy	1.78	2.02	1.81	1.83	1.82	2.08	2.17	1.96	1.91
Ho	0.28	0.32	0.28	0.29	0.28	0.33	0.34	0.31	0.30
Er	1.07	1.06	1.07	1.04	0.95	1.18	1.13	1.07	1.15
Tm	0.100	0.11	0.097	0.09 9	0.10	0.12	0.12	0.11	0.11
Yb	0.60	0.68	0.60	0.60	0.60	0.69	0.74	0.69	0.66
Lu	0.093	0.10	0.092	0.09 1	0.090	0.11	0.11	0.10	0.100
Σ REE	270.0 3	283.5 0	263.5 6	299. 68	251.8 4	298.9 0	287.7 1	298.44	326.40
LREE	259.6 7	272.1 6	253.1 4	288. 78	241.9 4	287.3 5	276.0 0	287.19	314.88
HREE	10.36	11.34	10.42	10.9 0	9.90	11.55	11.71	11.25	11.52
LaN/YbN	81.23	74.82	78.80	92.3 2	74.80	79.74	68.24	78.37	93.96
LaN/SmN	7.10	6.68	6.76	7.74	6.60	7.11	6.20	6.99	8.08

In the original mantle standardization diagram, the samples Nb, Ce, Zr and Ti have negative anomalies, while Pb has positive anomalies (FIG. 7). Sr= $1817 \times 10^{-6} \sim 2017 \times 10^{-6}$  (mean  $1915 \times 10^{-6}$ ); Yb= $0.60 \times 10^{-6} \sim 0.74 \times 10^{-6}$  (mean  $0.68 \times 10^{-6}$ ), with high Sr and low Yb characteristics. Nb= $5.58 \times 10^{-6} \sim 7.13 \times 10^{-6}$  (mean  $6.23 \times 10^{-6}$ ), Ta= $0.35 \times 10^{-6} \sim 0.46 \times 10^{-6}$  (mean  $0.40 \times 10^{-6}$ ), Nb/Ta=14.67~16.73 (mean 15.54), Nb/Ta ratio close to continental crust (continental crust Nb/Ta=11.36)<sup>[31]</sup>.



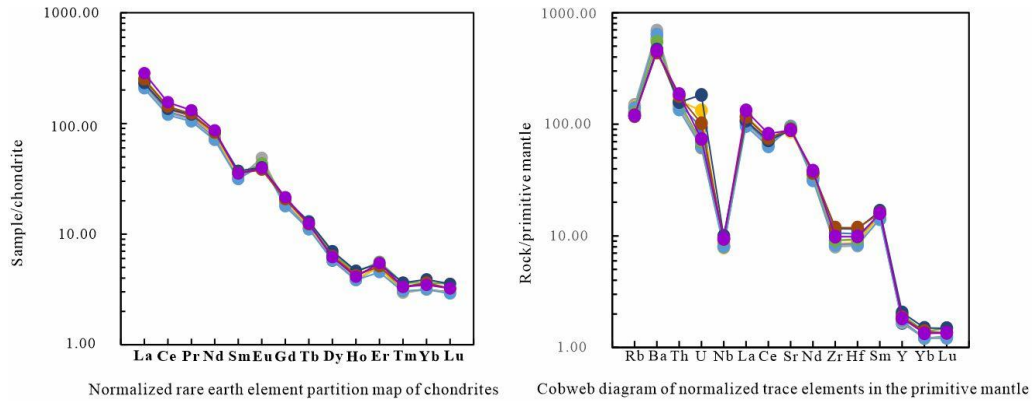


Fig. 7 Distribution curves of trace elements and rare earth elements in Dellancun porphyritic granite<sup>[32-33]</sup>

## 5. Discuss

### 5.1 Rock Genesis

The porphyritic granite in Dellanvillage belongs to the high potassium calc-alkaline rock series of quasi-aluminium-peraluminous rocks (FIG. 6). The A/CNK values range from 0.89 to 1.06, and are all less than 1.1. High field strength elements Nb, Ta and Ti all show losses, indicating that it belongs to type I granite<sup>[34-36]</sup>, light and heavy rare earth elements are obviously different, Y/Yb=12.26-13.22, (Er/Lu)<sub>N</sub>=0.77-1.79, heavy rare earth elements are not obviously different. In the diagrams of 10000×Ga/Al-Zr and 10000×Ga/Al-Y, the samples are located in the region of type I and type S granite (FIG. 8), while in the diagrams of SiO<sub>2</sub>-Zr, the samples are all located in the region of type I granite (FIG. 8). In the diagrams of SiO<sub>2</sub>-P<sub>2</sub>O<sub>5</sub>, there is a negative correlation between SiO<sub>2</sub>-P<sub>2</sub>O<sub>5</sub>. It is in the range of evolution trend of type I granite (FIG 8). The La/Nb ratio of the samples ranges from 10.36 to 14.71, with an average of 12.33, which is higher than the La/Nb ratio of continental crust (La/Nb=1.24)<sup>[31]</sup>, further indicating that the Dellancun porphyry granite belongs to type I granite.

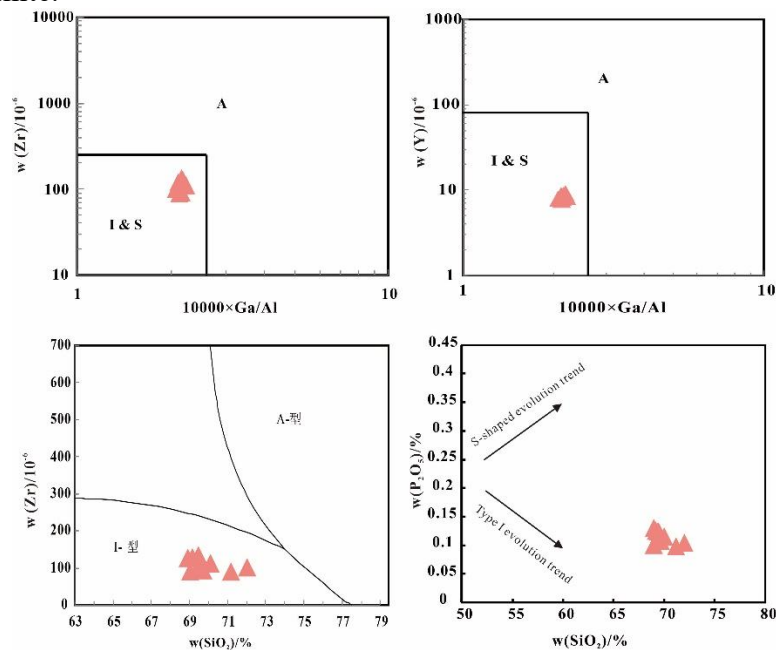


Fig. 8. Classification map of porphyritic granite in Dellan Village<sup>[37]</sup>

In the Y- (Sr/Y) diagram (FIG. 9a), the samples all fall within the Adakite region. In addition, the overall ratio of Sr/Y to La/Yb of porphyritic granite in Dalanvillage is high, Sr/Y=199.89~262.29, La/Yb=99.86~138.18, The high Sr (all greater than  $400 \times 10^{-6}$ ), low Yb (all less than  $1.9 \times 10^{-6}$ ) and low Y (all less than  $18 \times 10^{-6}$ ) geochemical characteristics are obvious, which is consistent with the results of previous studies on Yanshanian granites in eastern China<sup>[38-39]</sup>, and they should all belong to Adakite<sup>[40]</sup>.

It should be noted that there are obvious negative anomalies in Nb and Ti, and slight negative anomalies in Eu in the samples, suggesting that the magmatic source area of Dellancun porphyry granite may have been mixed with mantle-derived materials. In the diagrams of SiO<sub>2</sub>-MaO, SiO<sub>2</sub>-Ni and SiO<sub>2</sub>-Cr(FIG. 9b, c, d), most of the samples fall on the Adakite region under the background of the thickened lower crust and the subducted oceanic crust, while a few fall on the Adakite region with the origin of the thickened lower crust. It also indicates that the porphyrogranite magmatic source area in the study area suffered from mixing of lower crustal materials or subduction residual oceanic crust fluids<sup>[43]</sup>.

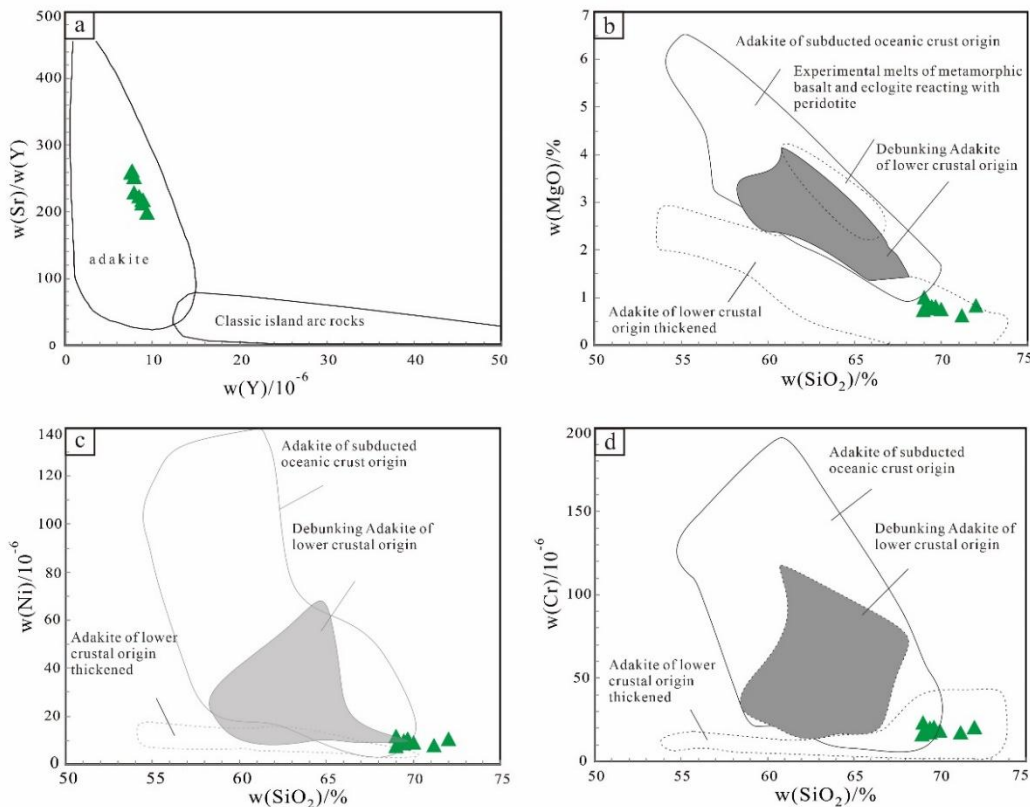


Fig. 9 Discriminant map of tectonic environment of porphyritic granite formation in Dellancun<sup>[41-42]</sup>

In the  $\delta\text{Eu} - (\text{La}/\text{Yb}) \text{ N}$  diagram (FIG. 10), the samples all fall in the crust-mantle granite region, which further indicates that the porphyritic granite parent magma in the study area may have been mixed by mantle materials during the evolution process. Combined with the typical Adakite geochemical characteristics of the samples, we suggest that the emplacement of Dalancun porphyritic granite magma is related to the subduction of the paleo-Pacific plate.

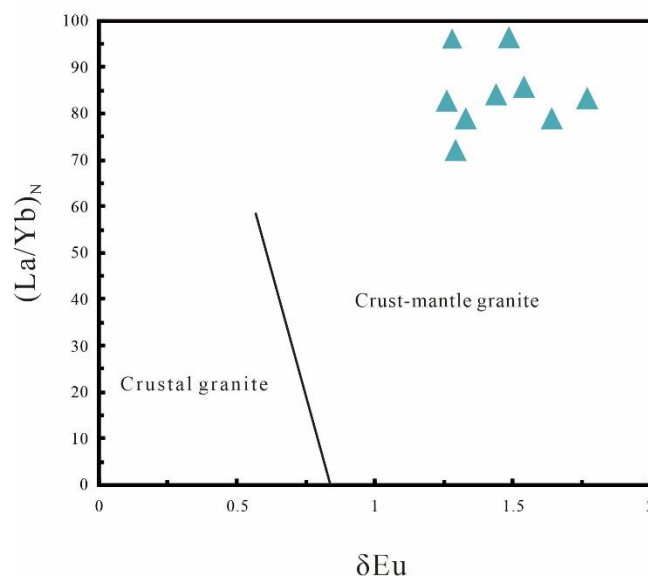


Fig. 10 Diagram of  $\delta\text{Eu}$ -  $(\text{La}/\text{Yb})_N$

## 5.2 Tectonic environment

Previous studies have suggested that since the Cretaceous, the subduction of the Pacific plate and the large-scale thinning of the North China Craton lithosphere have resulted in the Jiaodong area under the backarc stretching tectonic background [45]. Dalancun porphyritic granite is a type I granite of quasi-aluminium-peraluminous high potassium calc-alkaline series, which has geochemical characteristics of active continental margin granites [44]. In the discriminant map of Y-Nb tectonic environment (FIG. 11a), the samples all fall in the area of volcanic arc granite or syncollisional granite. In the  $(\text{Y}+\text{Nb})$ -Rb tectonic environment discriminant map (FIG. 11b), the samples all fall in the volcanic arc granite area, suggesting that the Dellancun porphyry granite may be formed in the active continental margin arc (continental margin arc), which is closely related to the subduction of the Pacific plate.

In addition, regional geological studies have shown that the Jiaodong area has strong Mesozoic magmatic activity, and the early Cretaceous granites in the study area are mainly represented by the Guojialing and Aishan plutons [44], and the parent magma has multi-source mixing characteristics [46]. The Dalancun porphyry granite belongs to the middle to late Early Cretaceous, which was formed in the period of the large scale thinning of the North China plate lithosphere, and is also an important period of the transformation of the lithosphere from compressive to extensional tectonic system in eastern China. This large-scale tectonic magmatic activity is related to the subduction of the Pacific plate to the Eurasian plate, resulting in strong magmatic activity in eastern China. In the late Mesozoic, regional stretching occurred in the North China Plate [47], resulting in a huge thinning of the lithosphere [48], which induced asthenosphere convection and promoted the development of local mantle plumes. Combined with the subduction fluid's transformation of mantle wedge and the warming and decompression, partial melting occurred in the metamorphic basement of the Jiaodong Group, and the mixing of crust source and mantle source components resulted in the formation of crust-mantle mixed magma, which invaded along crustal cracks and faults under the background of regional extension, resulting in multiple stages of magma intrusion events in the Jiaodong block [44], including the emplacing of Dellancun porphyritic granite.

It should be pointed out that the emplacement age and mechanism of Dalancun porphyritic granite are very similar to that of Guojialing porphyritic granite [11]. Therefore, during the formation of Dalancun porphyritic granite, it may also provide ore-forming materials, heat sources and mineralizing agents for Jiaodong gold deposit.

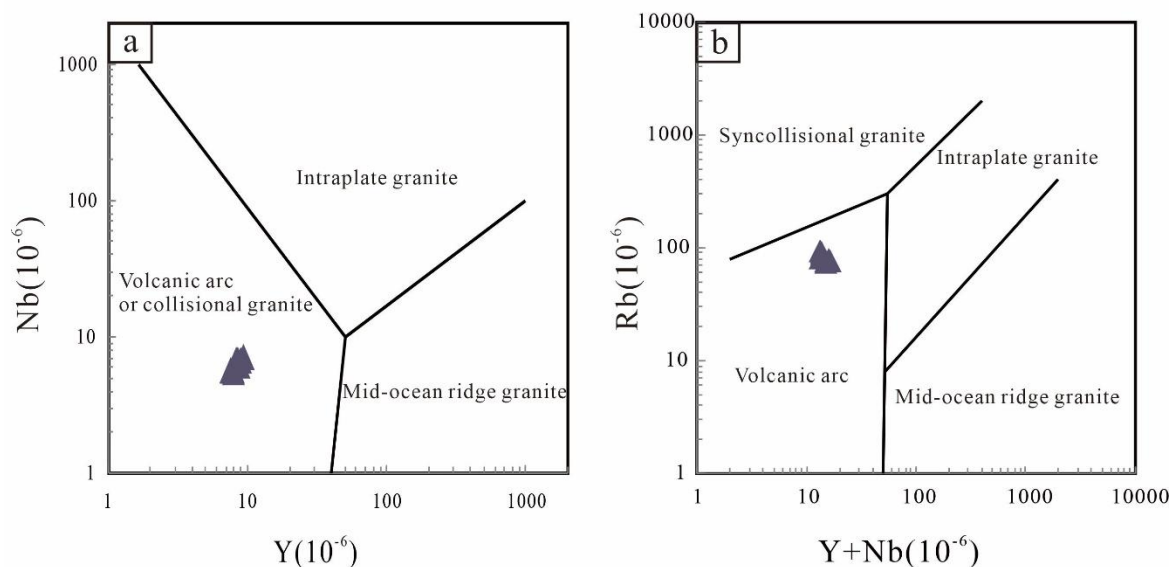


Fig. 11. Discrimination diagram of tectonic environment of Dellancun porphyry granite<sup>[23]</sup>

## 6. Conclusion

(1) The Dellancun porphyry granite is the product of early Cretaceous ( $129.7 \pm 0.8$  Ma) magmatic activity in Jiaodong area. It belongs to type I granite with typical Adakite geochemical characteristics. Its parent magma was contaminated by mantle-derived materials and belongs to crust-mantle mixed type.

(2) The Dalancun porphyry granite may have been formed in the arc environment of continental margin during the transition period from compressive to extensional tectonic system, which is closely related to the subduction of the paleo-Pacific plate.

(3) The emplacement process of Dalancun porphyritic granite may provide ore-forming materials, heat sources and mineralizing agents for Jiaodong gold deposit.

## 7. References

- [1] Xi Hong. Study on zircon characteristics of early Cretaceous granite in Jiaodong area and its constraints on gold mineralization [D]. Chinese Academy of Geological Sciences, 2020.
- [2] Wei Yuji, Qiu Kunfeng, Guo Linnan, et al. Characteristics and evolution of ore-forming fluid in Dayinggezhuang Gold Deposit, Jiaodong Province [J]. *Acta Petrologica Sinica*, 2020, 36(06): 1821-1832.
- [3] Fan Hongrui, Feng Kai, Li Xinghui, et al. Mesozoic gold mineralization in Jiaodong and Korean Peninsula [J]. *Acta Petrologica Sinica*, 2016, 32(10): 3225-3238.
- [4] Ma L, Jiang S Y, Dai B Z, et al. Multiple sources for the origin of Late Jurassic Linglong adakitic granite in the Shandong Peninsula, Eastern China: Zircon U-Pb geochronological, Geochemical and Sr-Nd-Hf isotopic evidence [J]. *Lithos*, 2013, 162-163: 251-263.
- [5] Huang T. Inherited Zircons from the Linglong Granite: Constraints on Pre-Mesozoic Crustal Evolution and Its Implications for Mesozoic Gold Mineralization in Jiaobei Terrane, China [J]. *Acta Geologica Sinica*, 2014, 88(22): 1624-1625.
- [6] Guo L N, Deng J, Yang L Q, et al. Gold deposition and resource potential of the Linglong gold deposit, Jiaodong Peninsula: Geochemical comparison of ore fluids [J]. *Ore Geology Reviews*, 2020, 120: 103434.
- [7] Meng F, Sun D, Li S. Characteristics and Metallogeny of Cishan Granite, East Shandong (Jiaodong) [J]. *Mineral Deposits*, 2001.

- [8] ZHANG Juan. Geochemistry of Mesozoic magmatic rocks in Sulu Orogenic belt [D]. Hefei: University of Science and Technology of China, 2011.
- [9] Liu Hongtao, Sun Shihua, Liu Jianming, et al. Mesozoic High Strontium granites in the northern margin of North China Craton: Geochemistry and provenance Properties [J]. *Acta Petrologica Sinica*, 2002, 18(3): 257-274.
- [10] The Formation age, genesis and Geological significance of Dupangling Ring porphyry granite [J]. *Geotectonics and Metallogeny*, 2017, 41(03): 561-576. (in Chinese)
- [11] Chen Guangyuan, Sun Daisheng, Zhou Shenruo, et al. Genetic mineralogy and gold mineralization of Guojialing granodiorite in Jiaodong [M]. Beijing: China University of Geosciences Press, 1993, 1-230.
- [12] Zhang Tian, Zhang Yueqiao. *Geological Journal of China Universities*, 2007(02): 323-336.
- [13] Wang Laiming, Ren Tianlong, Liu Handong, et al. Division of Mesozoic granites in Jiaodong Area [J]. *Shandong Land and Resources*, 201, 37 (8) : 1-14.
- [14] Lin Bo-lei, Li Bi-le. Geochemistry, U-Pb chronology, Lu-Hf Isotopes and their Geological Significance of Linglong granites in Jiaodong [J]. *Journal of Chengdu University of Technology (Science & Technology Edition)*, 2013, 40(02): 147-160.
- [15] Du Zezhong, Cheng Zhizhong, Yao Xiaofeng, et al. The  $(40)\text{Ar}\sim(39)\text{Ar}$  age and its Geological Significance of altered potassium feldspar in Xiejiagou Gold Deposit, Jiaodong Province [J]. *Journal of Jilin University (Earth Science Edition)*, 2020, 50(05): 1570-1581.
- [16] Li Hailin. Alteration and mineralization network structure of Luoshan gold Deposit, Northwest China [D]. China University of Geosciences (Beijing), 2015.
- [17] Yang Liqiang, Deng Jun, Wang Zhongliang, et al. Mesozoic gold metallogenic system in Jiaodong [J]. *Acta Petrologica Sinica*, 2014, 30(09): 2447-2467. Li Junjian, Luo Zhenkuan, Liu Xiaoyang, et al. Study on the Geochemical Characteristics of Gold Deposit in Shandong Province [J]. *Mineral Deposits*, 2005(04): 361-372.
- [18] Li Zhaolong, Yang Minzhi. *Geology and Geochemistry of Jiaodong Gold Deposit* [M]. Tianjin Science and Technology Press, 1993.
- [19] Feng Qiao, Xu Zisu, Zhang Yao, et al. Zircon U-Pb chronology of Early Cretaceous granites in Xiaozhushan, Jiaonan Uplift Zone, Qingdao and genesis of Mesozoic granites in Jiaodong Peninsula [J]. *Journal of Shandong University of Science and Technology (Natural Science Edition)*, 2019, 38(2): 1-13.
- [20] Hu Z ,Gao S ,Liu Y , et al. Signal enhancement in laser ablation ICP-MS by addition of nitrogen in the central channel gas[J]. *Journal of Analytical Atomic Spectrometry*, 2008, 23(8): 1093-1101.
- [21] Liu Y S, Hu Z C, Zong K Q, et al. Reappraisal and refinement of zircon U-Pb isotope and trace element analyses by LA-ICP-MS[J]. *Science bulletin: English version*, 2010(15): 12.
- [22] Liu Y, Hu Z, Gao S, et al. In situ analysis of major and trace elements of anhydrous minerals by LA-ICP-MS without applying an internal standard[J]. *Chemical Geology*, 2008, 257(1): 34-43.
- [23] Liu Y S. Continental and Oceanic Crust Recycling-induced Melt-Peridotite Interactions in the Trans-North China Orogen: U-Pb Dating, Hf Isotopes and Trace Elements in Zircons from Mantle Xenoliths[J]. *Journal of Petrology*, 2010, 51(1-2): 537-571.
- [24] Ludwig K R. ISOPLOT a Plotting and Regression Program for Radiogenic-isotope Data[J]. Open-File Report, 1994.
- [25] Zhou Jianbo, Zheng Yongfei, Zhao Zifu. Zircon U-Pb ages of Mesozoic magmatic rocks in Wulian, Shandong Province [J]. *Geological Journal of China Universities*, 2003(02): 185-194.
- [26] Liu Xiaoming, Gao Shan, Wu Chunrong, Yuan Honglin, Hu Zhaochu. Simultaneous Determination of LA-ICP-MSU-Pb Age and Trace Elements in in-situ micro-region of  $20\mu\text{m}$  small spot beam of single zircon [J]. *Journal of Science General*, 2007(02): 228-235.
- [27] Peccerillo R, Taylor S R. Geochemistry of eocene calc-alkaline volcanic rocks from the Kastamonu area, Northern Turkey. *Contrib. Mineral Petrol.*, 1976, 58: 63~81.
- [28] Middlemost E A K. *Magmas and Magmatic Rocks*. London: Longman, 1985, 1~266.
- [29] Middlemost E A K. Naming materials in the magma/igneous rock system[J]. *Earth Science Reviews*, 1994, 37(3-4): 215-224.

- [30] Maniar PD, Piccoli PM. Tectonic discrimination of granitoids[J]. Geological Society of America Bulletin, 1989, 101(5): 635-643.
- [31] Taylor S R, Mclenman S M. 1985. The Continental Crust: Its Composition and Evolution: An Examination of the Geochemical Record Preserved in Sedimentary Rocks[M]. Oxford: Blackwell Scientific Publications, 1-301.
- [32] Effects of different average values of Chondrites on rare earth element parameters [J]. Standardization Report, 2000, 21(3): 15-16. (in Chinese)
- [33] Sun S-S, McDonough WF. 1989. Chemical and isotopic systematics of oceanic basalts: implications for mantle composition and processes. In: Saunders, A.D., Norry, M.J. (Eds.), Magmatism in the Ocean Basins. Geological Society London. Special Publications, vol. 42, pp. 313 -- 345.
- [34] Bai Xianzhou. Study on Geology and geochemistry of granite in Longling Area, western Yunnan and its mineralization [D]. Chengdu University of Technology, 2014.
- [35] Wu Yuanbao, Zheng Yongfei. Zircon genetic mineralogy and its restriction on U-Pb age interpretation. Chinese Science Bulletin, 2004, (16): 1589-1604.
- [36] Zhang L, Wang P, Chen X, et al. Acquisition, analysis and comparison of detrital zircon U-Pb chronology data [J]. Advances in Earth Science, 2020, 35(04): 414-430.
- [37] Whalen J B, Currie K L, Chappell B W. A-type granites: geochemical characteristics, discrimination and petrogenesis. Contributions to Mineralogy and Petrology, 1987, 95: 407-419.
- [38] Ge Xiaoyue, Li Xianhua, Chen Zhigang, et al. Geochemical characteristics and genesis of Yanshanian high Sr low Y type medium acid igneous rocks: Constraints on crustal thickness in eastern China [J]. Chinese Science Bulletin, 2002(06): 474-480.]
- [39] Liu Hongtao, Sun Shihua, Liu Jianming, et al. Mesozoic High strontium granites in the northern margin of North China: geochemistry and provenance properties [C]. Institute of Geology and Geophysics, Chinese Academy of Sciences, 2002: 208-209.
- [40] W. J. Collins, S. D. Beams, A. J. R. White, et al. Nature and origin of A-type granites with particular reference to southeastern Australia[J]. Contributions to Mineralogy and Petrology, 1982, 80(2).
- [41] Defant M J, Drummond M S. Derivation of some modern arc magmas by melting of young subducted lithosphere[J]. Nature, 1990, 347(6294): 662-665.
- [42] Wang Q. Petrogenesis of Adakitic Porphyries in an Extensional Tectonic Setting, Dexing, South China: Implications for the Genesis of Porphyry Copper Mineralization[J]. Journal of Petrology, 2006, 47(1): 119 -144.
- [43] J. Godfrey Fitton, Dodie James, William P. Leeman. Basic magmatism associated with Late Cenozoic extension in the western United States: Compositional variations in space and time[J]. John Wiley & Sons, Ltd, 1991, 96(B8).
- [44] Han Zongzhu, Zhang He, Tian Yuan, et al. Petrogeochemical characteristics and genesis of Asanshan granodiorite in Qixia, Shandong Province [J]. Journal of Ocean University of China (Natural Science Edition), 2011, 41(06): 97-103.
- [45] Zou Jian, Tang Wenlong, Ding Zhengjiang, et al. Zircon U-Pb Age of Yuangezhuang Pluton in Muping, Shandong Province and its Influence on the Metallogenic Regularity of Cu-Mo polymetal [J]. Geology in China, 2021, 48(03): 883-899.
- [46] Wu Fuyuan, Li Xianhua, Yang Jinhui, et al. Some problems in the study of granite genesis [J]. Acta Petrologica Sinica, 2007(06): 1217-1238.
- [47] Guo Chunli, Wu Fuyuan, Yang Jinhui, et al. Extensional tectonic properties of Early Cretaceous magmatism in Eastern China: A case study of Yinmawanshan pluton, southern Liaodong Peninsula [J]. Acta Petrologica Sinica, 2004(05): 204-215.
- [48] Wang Feifei, Han Zongzhu, Zhang Yong, et al. Geochemical characteristics and genesis of Ashan granite and its dark inclusions in Qixia [J]. Collection of Geological Prospecting Papers, 2019, 34(03): 393-405.